# Evolution of the concept of Quark Matter

## The Ianus face of Quark Matter

a subjective view

## God of beginnings and endings

## COLLISION

color glass condensate? (M. Gyulassy, L. McLerran, 2005)

## QGP formation ?

transfer from high to low momenta (G.L.V. 2000)

## EVOLUTION of PLASMA

expands and cools, undergoes through a set of phases

## PREHADRONIZATION STAGE

quarks and antiquarks gather effective mass (P.Lévai, U.Heinz, 1996)

## HADRONIZATION

quarks and antiquarks coalesce into hadrons (ALCOR, 1995)

IN HEAVY ION COLLISIONS

NOT A SINGLE SORT,

WELL DEFINED TYPE OF MATTER IS FORMED

BUT A SET OF DIFFERENT TYPE OF MATTER

IS CREATED

IN THE CONSECUTIVE STAGES OF THE REACTION

# Evolution of the concept of Quark Matter (1)

Ed Shuryak, 1980

| microstructure of QM | bulk properties of QM |
| --- | --- |
| very high quark density; | static, homogeneous gas; |
| Fermi levels occupied | very high temperature; |
| up to very high momenta; | sound velocity vanishing; |
| coupling constant vanishing; | long lifetime; |
| zero effective mass | |
| of quarks and gluons; | |

# Evolution of the concept of Quark Matter (2)

| microstructure of QM | bulk properties of QM |
| --- | --- |
| not too high quark density; | fast expansion ; |
| coupling constant | temperature near to critical; |
| not vanishing; | short lifetime; |
| finite effective mass | |
| of quarks and gluons; | strongly interacting constituents; |

## Evolution of the concept of hadronization (1)

thermodynamical first order phase transition;

mixed phase transition;

coalescence

# Evolution of the concept of coalescence (1)

number conservation in coalescence;

simple quark counting;

linear vs. nonlinear coalescence;

momentum conservation in coalescence;

mass conservation in coalescence

# Coalescence hadronization with constituent quark number conservation

(J. Zimányi, P. Lévai and T.S. Biró, 1995)

For the description of hadrons the constituent quark model was quite successfull. In this approach the quarks are dressed, with mass of approximatively $300 MeV$. The question arises, that at what stage of hadronization is crated this effective mass? In the ALCOR model (ALgebraic COmbinatoric Rehadronization) it is assumed, that this effective mass is created in the very last stage of the evolution of fireball.

## The main assumptions of the ALCOR model.

**At the beginning of hadronization the quarks are dressed constituent quarks.**

These quarks coalesce to form the hadrons.

**The number of different quarks and anti-quarks is conserved during hadronization.**

The effective mass of gluons is much higher than that of quarks near the critical temperature. Thus the gluon degree of freedom is neglected in this late period of the heavy ion reaction.

The number of a given type of hadron is propor-tianal to the product of the numbers of different quarks from which the hadron consists.

In the linear coalescence model

**the subprocesses are independent,**

In the nonlinear ALCOR coalescence model

**the subprocesses are not independent,**

**they compete with each other.**

# The coalescence equations

In order to make this definition transparent, first we display its consequences for the the case, where the up and down quarks are assumed to be the same: $u = d$, $u + d = q$.

The essence of the ALCOR model will be approximated by an oversimplified situation. Let us assume, that in the quark phase we have $N_q^{in}$ and $N_s^{in}$ number light and strange quarks. In the hadron phase the number of these quarks are $N_q^{out}$ and $N_s^{out}$. Further in the hadronic phase we have only protons and $\Lambda$ particles. Then the coalescence equation reads as

$$N_p = \frac{C_p}{V * V}(b_q \cdot N_q^{in}) * (b_q \cdot N_q^{in}) * (b_q \cdot N_q^{in})$$

$$N_\Lambda = \frac{C_\Lambda}{V * V}(b_q \cdot N_q^{in}) * (b_q \cdot N_q^{in}) * (b_s \cdot N_s^{in})$$

We demand

$$N_q^{out} = N_q^{in} = N_q$$

$$N_s^{out} = N_s^{in} = N_s$$

Thus the balance equations are:

$$\begin{aligned} N_q &= 3 * N_p + 2 * N_\Lambda \\ N_s &= N_\Lambda \end{aligned} \tag{1}$$

Substituting the expressions for the proton and $\Lambda$ production we get the equations defining the $b_q$ and $b_s$ normalization coefficients:

$$\begin{aligned} N_q &= 3 * \frac{C_p}{V * V}(b_q \cdot N_q) * (b_q \cdot N_q) * (b_q \cdot N_q) \\ &+ 2 * \frac{C_\Lambda}{V * V}(b_q \cdot N_q) * (b_q \cdot N_q) * (b_s \cdot N_s) \\ N_s &= \frac{C_\Lambda}{V * V}(b_q \cdot N_q) * (b_q \cdot N_q) * (b_s \cdot N_s) \end{aligned}$$

Notation: $q = N_q/V$. The baryon productions:

$$\begin{aligned} \mathbf{p} &= \mathbf{C_p\, b_q\, b_q\, b_q\, q\, q\, q} \\ \mathbf{\Lambda} &= \mathbf{C_\Lambda\, b_q\, b_q\, b_s\, q\, q\, s} \\ \mathbf{\Xi} &= \mathbf{C_\Xi\, b_q\, b_s\, b_s\, q\, s\, s} \\ \mathbf{\Omega} &= \mathbf{C_\Omega\, b_s\, b_s\, b_s\, s\, s\, s} \end{aligned} \tag{2}$$

We obtain similarly the antibaryons:

$$\begin{aligned} \overline{\mathbf{p}} &= \mathbf{C_{\overline{p}}\, b_{\overline{q}}\, b_{\overline{q}}\, b_{\overline{q}}\, \overline{q}\, \overline{q}\, \overline{q}} \\ \overline{\mathbf{\Lambda}} &= \mathbf{C_{\overline{\Lambda}}\, b_{\overline{q}}\, b_{\overline{q}}\, b_{\overline{s}}\, \overline{q}\, \overline{q}\, \overline{s}} \\ \overline{\mathbf{\Xi}} &= \mathbf{C_{\overline{\Xi}}\, b_{\overline{q}}\, b_{\overline{s}}\, b_{\overline{s}}\, \overline{q}\, \overline{s}\, \overline{s}} \\ \overline{\mathbf{\Omega}} &= \mathbf{C_{\overline{\Omega}}\, b_{\overline{s}}\, b_{\overline{s}}\, b_{\overline{s}}\, \overline{s}\, \overline{s}\, \overline{s}} \end{aligned} \tag{3}$$

Finally the mesons:

$$\begin{aligned} \pi &= \mathbf{C}_\pi \, \mathbf{b}_{\mathrm{q}} \, \mathbf{b}_{\overline{\mathrm{q}}} \, \mathbf{q} \, \overline{\mathbf{q}} \\ \mathbf{K} &= \mathbf{C}_{\mathbf{K}} \, \mathbf{b}_{\mathrm{q}} \, \mathbf{b}_{\overline{\mathrm{s}}} \, \mathbf{q} \, \overline{\mathbf{s}} \\ \overline{\mathbf{K}} &= \mathbf{C}_{\overline{\mathbf{K}}} \, \mathbf{b}_{\overline{\mathrm{q}}} \, \mathbf{b}_{\mathrm{s}} \, \overline{\mathbf{q}} \, \mathbf{s} \\ \eta &= \mathbf{C}_\eta \, \mathbf{b}_{\overline{\mathrm{s}}} \, \mathbf{b}_{\mathrm{s}} \, \overline{\mathbf{s}} \, \mathbf{s} \end{aligned} \tag{4}$$

The normalization coefficients, $b_{\mathrm{i}}$, are determined uniquely by the requirement, that the number of the constituent quarks do not change during the hadronization

$$
\begin{aligned}
\mathbf{s} &= \mathbf{3\,\Omega + 2\,\Xi + \Lambda + \overline{K}} + \eta \\
\overline{\mathbf{s}} &= \mathbf{3\,\overline{\Omega} + 2\,\overline{\Xi} + \overline{\Lambda} + K} + \eta \\
\mathbf{q} &= \mathbf{3\,p + \Xi + 2\,\Lambda + K} + \pi \\
\overline{\mathbf{q}} &= \mathbf{3\,\overline{p} + \overline{\Xi} + 2\,\overline{\Lambda} + \overline{K}} + \pi\ .
\end{aligned}
\tag{5}
$$

Substituting eqs. (3-4) into eq. (5) one obtains equations for the normalization constants.

| | ALCOR model | Preliminary data | Ref. |
|---|---|---|---|
| $h^-$ | 280 | $280 \pm 20$ | STAR (12) |
| $K^-/\pi^-$ | 0.14 | $0.15 \pm 0.01$ | STAR (13) |
| $K^+/K^-$ | 1.14 | $1.14 \pm 0.06$ | STAR (13) |
| $\overline{p}^-/p^+$ | 0.63 | $0.60 \pm 0.03$ | STAR (13) |
| $\overline{\Lambda}/\Lambda$ | 0.73 | $0.73 \pm 0.03$ | STAR (13) |
| $\overline{\Xi}^+/\Xi^-$ | 0.83 | $0.82 \pm 0.08$ | STAR (13) |
| $\Xi^-/\pi^-$ | 0.015 | $0.013 \pm 0.01$ | STAR (14) |
| $\Phi/K^{*0}$ | 0.38 | $0.49 \pm 0.13$ | STAR (15) |
| $\overline{p}/h^-$ | 0.087 | $0.070 \pm 0.002$ | STAR (16) |

Table 1: Hadron production in Au+Au collision at $\sqrt{s} = 130$ AGeV from the ALCOR model and the preliminary experimental data. Red numbers are the input data.

# The simple quark counting

(linear quark counting, A.Bialas, (1999))
(non linear quark counting J.Zimányi, T.S.Biró, T.Csörgö, P.Lévai,(2000))

Realizing that

$$C_h = C_{\overline{h}}, \tag{6}$$

very transparent relations can be obtained for the ratios of the different multiplicities:

$$
\begin{aligned}
\frac{\overline{\mathrm{p}}}{\mathrm{p}} &= \frac{b_{\overline{q}}\, b_{\overline{q}}\, b_{\overline{q}}\, \overline{q}\,\overline{q}\,\overline{q}}{b_q\, b_q\, b_q\, q\, q\, q} \\
\frac{\overline{\Lambda}}{\Lambda} &= \frac{b_{\overline{q}}\, b_{\overline{q}}\, b_{\overline{s}}\, \overline{q}\,\overline{q}\,\overline{s}}{b_q\, b_q\, b_s\, q\, q\, s} = \frac{b_q\, b_{\overline{s}}\, q\, \overline{s}}{b_{\overline{q}}\, b_s\, \overline{q}\, s} \cdot \frac{\overline{\mathrm{p}}}{\mathrm{p}} \\
\frac{\overline{\Xi}}{\Xi} &= \frac{b_{\overline{q}}\, b_{\overline{s}}\, b_{\overline{s}}\, \overline{q}\,\overline{s}\,\overline{s}}{b_q\, b_s\, b_s\, q\, s\, s} = \frac{b_q\, b_{\overline{s}}\, q\, \overline{s}}{b_{\overline{q}}\, b_s\, \overline{q}\, s} \cdot \frac{\overline{\Lambda}}{\Lambda} \\
\frac{\overline{\Omega}}{\Omega} &= \frac{b_{\overline{s}}\, b_{\overline{s}}\, b_{\overline{s}}\, \overline{s}\,\overline{s}\,\overline{s}}{b_s\, b_s\, b_s\, s\, s\, s} = \frac{b_q\, b_{\overline{s}}\, q\, \overline{s}}{b_{\overline{q}}\, b_s\, \overline{q}\, s} \cdot \frac{\overline{\Xi}}{\Xi} \qquad (7)
\end{aligned}
$$

The common factor appearing on the right hand side of equations (7) is

$$\mathbf{D} = \frac{\mathbf{b_q\, b_{\bar{s}}\, q\, \bar{s}}}{\mathbf{b_{\bar{q}}\, b_s\, \bar{q}\, s}} = \frac{\mathbf{K}}{\overline{\mathbf{K}}} \tag{8}$$

Thus one can write eq.7 in the simple form

$$\begin{aligned} \frac{\overline{\mathbf{\Lambda}}}{\mathbf{\Lambda}} &= \mathbf{D} \cdot \frac{\overline{\mathbf{p}}}{\mathbf{p}} \\ \frac{\overline{\mathbf{\Xi}}}{\mathbf{\Xi}} &= \mathbf{D} \cdot \frac{\overline{\mathbf{\Lambda}}}{\mathbf{\Lambda}} \\ \frac{\overline{\mathbf{\Omega}}}{\mathbf{\Omega}} &= \mathbf{D} \cdot \frac{\overline{\mathbf{\Xi}}}{\mathbf{\Xi}} \end{aligned} \tag{9}$$

| RATIOS | STAR | SPS |
|---|---|---|
| $K^+/K^-$ | $1.092 \pm 0.023$ | $1.76 \pm 0.06$ |
| $\{\overline{\Lambda}/\Lambda\}/\{\overline{p}/p\}$ | $0.98 \pm 0.09$ | $2.07 \pm 0.21$ |
| $\{\overline{\Xi}/\Xi\}/\{\overline{\Lambda}/\Lambda\}$ | $1.17 \pm 0.11$ | $1.78 \pm 0.15$ |
| $\{\overline{\Omega}/\Omega\}/\{\overline{\Xi}/\Xi\}$ | $1.14 \pm 0.21$ | $1.42 \pm 0.22$ |

Table 2: Compilation of experimetal particle ratios obtained at RHIC and SPS at energies $\sqrt{s} = 130$ GeV and 18 Gev, respectively. (STAR, nucl-ex/0211024 )

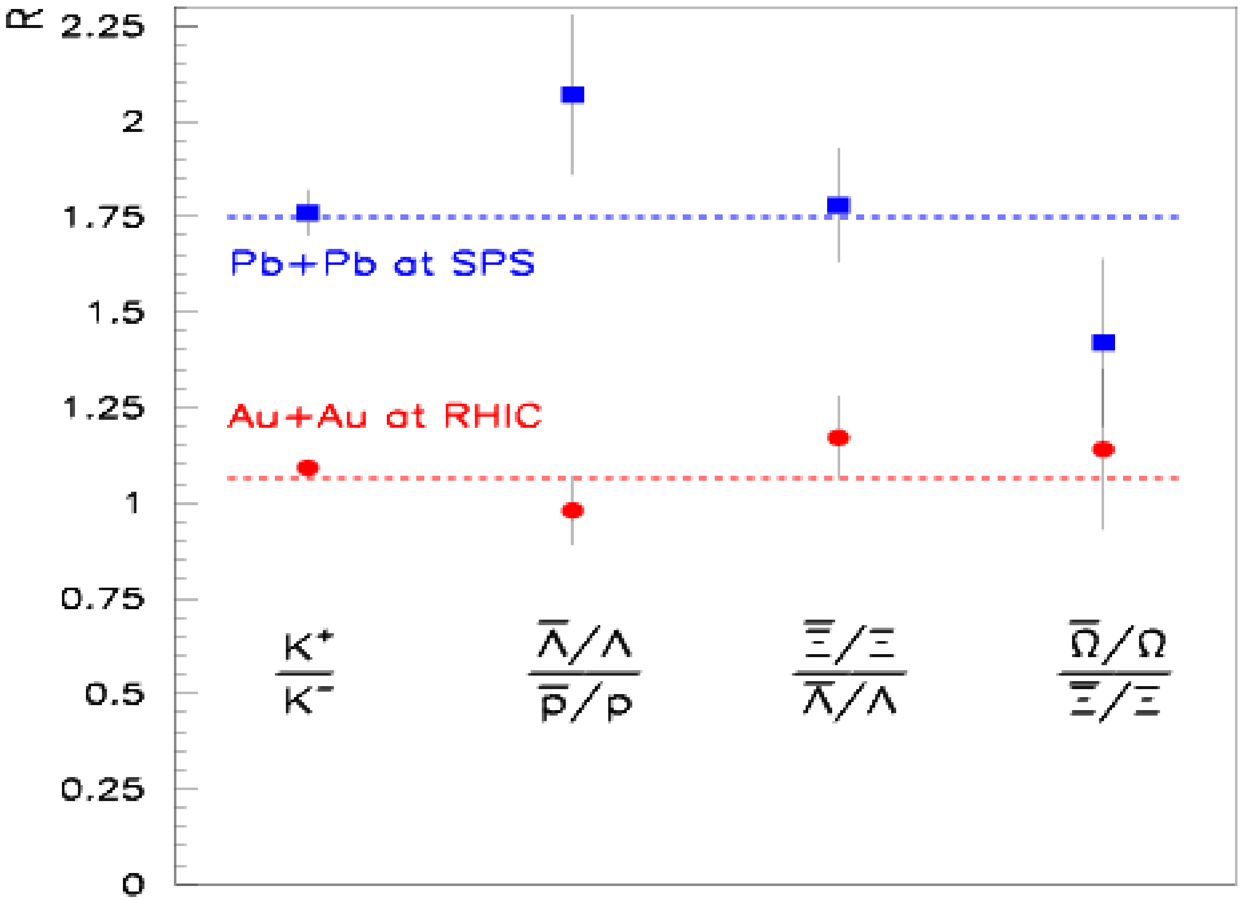


Figure 1: Graphical display of the particle ratios at mid-rapidity in Pb+Pb collisions at SPS and in Au+Au collision at RHIC. (Compilation by STAR experiment, nucl-ex/0211024 .)

# CHARGE FLUCTUATION IN A QUARK-ANTIQUARK SYSTEM

(A.Bialas )

In a recent paper [A.Bialas] interesting observation was made on the problem of charge fluctuation. Earlier M.Asakawa et al.(2000) suggested, that the ratio

$$D = 4\frac{< \delta Q^2 >}{< N_{ch} >} \qquad (10)$$

is approximately $D \approx 3$ for hadron gas in equilibrium, and $D \approx 1$ for the quark gluon plasma. $< \delta Q^2 >$ is the average of the charge fluctuation and $< N_{ch} >$ is the average value of the charge multiplicity. The measured $D$ value is near to 3.

That would indicate that in the heavy ion reactions no quark - gluon plasma, but a hadron gas was produced.

A.Bialas, however, did show , that in the coalescence scenario (ALCOR) one can also expect a $D \approx 3$ value. Thus one can conclude that the measured charged fluctuation is also in agreement with the basic assumption of the ALCOR, i.e. during the hadronization the number of constituent quarks and also the number of constituent antiquarks are conserved.

# Coalescence hadronization with constituent quark momentum conservation

R.Hwa, C.B.Yang, (2003)
V.Greco, C.M.Ko, P.Lévai, (2003)
R. J. Fries, S. A. Bass, B. Müller, C. Nonaka, (2003)

Using notation of R.Fries et al. and restric ourself to the region

$$p_{constituent\ quark} >> m_{constituent\ quark} \tag{1}$$

and with the assumpton

$$p_1 = p_2 = P_h/2 \tag{2}$$

Under this conditions the expression for the meson emission spectrum:

$$E\frac{dN_M}{d^3P} = \int_{\Sigma_f} d\sigma \, \frac{P \cdot u(r)}{(2\pi)^3} \, w_a(r; \frac{P}{2}) \, w_b(r; \frac{P}{2}) \, . \tag{3}$$

A similar expression for the baryon emission spectrum:

$$E\frac{dN_B}{d^3P} = \int_{\Sigma_f} d\sigma \, \frac{P \cdot u(r)}{(2\pi)^3} \, w_a(r; \frac{P}{3}) \, w_b(r; \frac{P}{3}) \, w_c(r; \frac{P}{3}). \tag{4}$$

These two equations lead to an interseting consequence:

since the momentum distribution of constituent quarks is expected to behave as an exponentialy decreasing function of trasverse momentum, there are more partons at $P/3$ than at $P/2$.

$$w_q(r; \frac{P}{3}) > w_q(r; \frac{P}{2}) \tag{5}$$

From that follows, that we have

more baryons than mesons

at the momentum range of hadrons produced by coalescence.

The predictions are radically different, when one considers a power law spectrum as it is characteristic in perturbative QCD at large transverse momentum:

$$w_a^{pert}(r;p) = A_a \left(1 + \frac{p_T}{B}\right)^{-\alpha} . \qquad (6)$$

Mesons always dominate over baryons at large momentum, and that parton fragmentation wins out over quark recombination. On the other hand, for an exponential quark spectrum, fragmentation is always suppressed with respect to recombination.

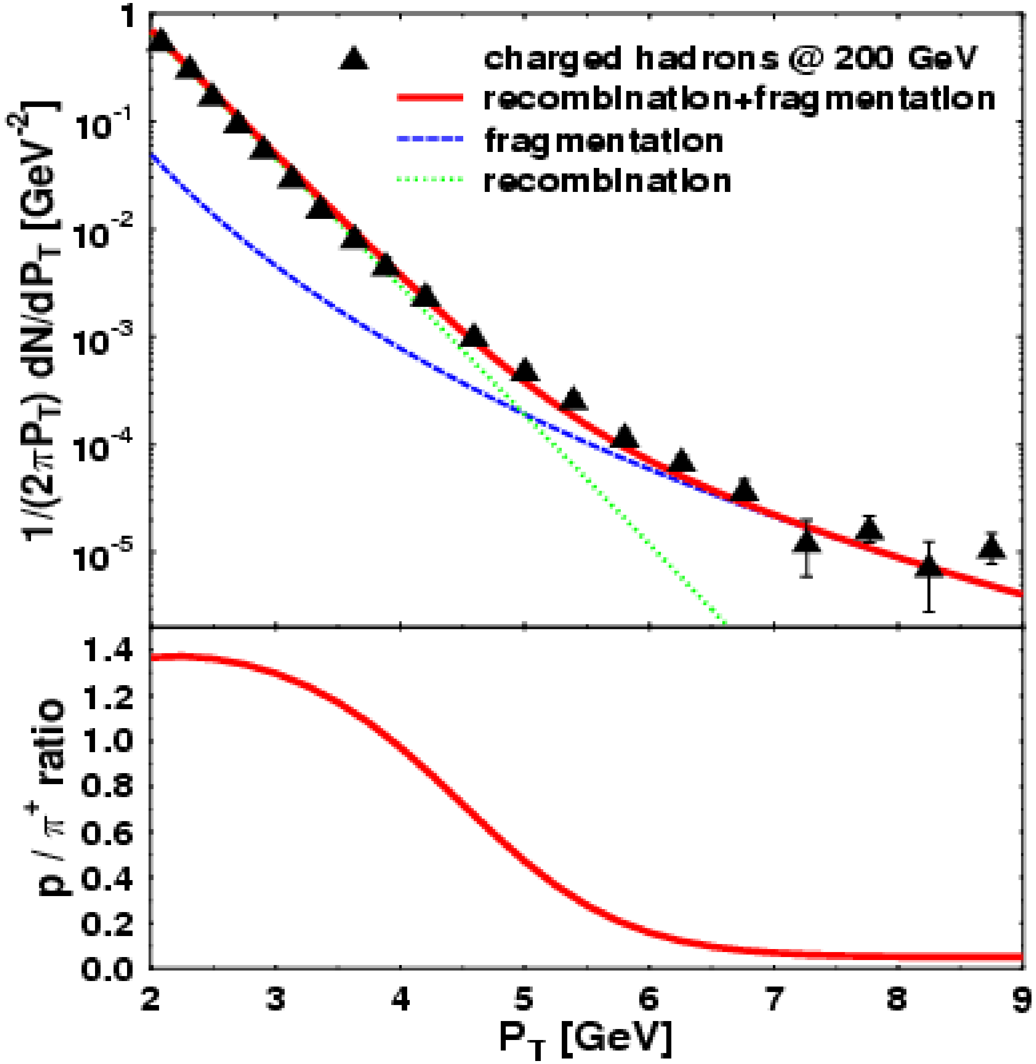
charged hadrons @ 200 GeV
recombination+fragmentation
fragmentation
recombination
$1/(2\pi P_T)\ dN/dP_T\ [GeV^{-2}]$
$p / \pi^+$ ratio
$P_T$ [GeV]

Conclusion:

Hadron emission from a thermal parton ensemble is *always* dominated by parton recombination; only when the thermal distribution gives way to a perturbative power law at high momentum, does fragmentation become the leading hadronization mechanism. The threshold between the two domains depends on the size of the emitting system and the hadron species.

# Properties of quark matter produced in heavy ion collision

J. Zimányi, P. Lévai, T.S. Biró

**The most important aim of heavy ion experiments performed at the RHIC accelerator besides the production of quark matter is the reconstruction of its properties from the observed hadron measurables.**

Three questions:

a) **the effective mass of the quarks,**
b) **the momentum distribution of quarks,**
c) **the hadronization mechanism.**

Mass of quark:

i) the quark matter consists of an ideal gas of non-interacting massless quarks and gluons and this type of quark matter undergoes a first order phase transition during the hadronization;

ii) the effective degrees of freedom in quark matter are dressed quarks with an effective mass of about 0.3 GeV, which mass is the result of the interactions within the quark matter; this type of quark matter clusterizes and forms hadrons smoothly, following a cross-over type deconfinement – confinement transition.

## Mass distribution of Quarks

The effective mass of quarks are determined by the neighborhood of the quark.

The matter in the fireball is not smooth and homogeneous. More probably it consists of granulates, in space and time, having different size and densities.

The granulated structure of the fireball is reflected in the effective mass distribution of the quarks.

**Presently we consider the following mass distribution:**

$$\rho(\mathbf{m}) = N\mathbf{e}^{-\frac{\mu}{\mathbf{T_c}}\sqrt{\frac{\mu}{\mathbf{m}}+\frac{\mathbf{m}}{\mu}}} \qquad (1)$$

**with** $\mu = 0.20$ **and** $0.25 GeV$ **and** $T_c = 0.26 GeV$**.**

From this distribution the effective mass of quarks is never negative

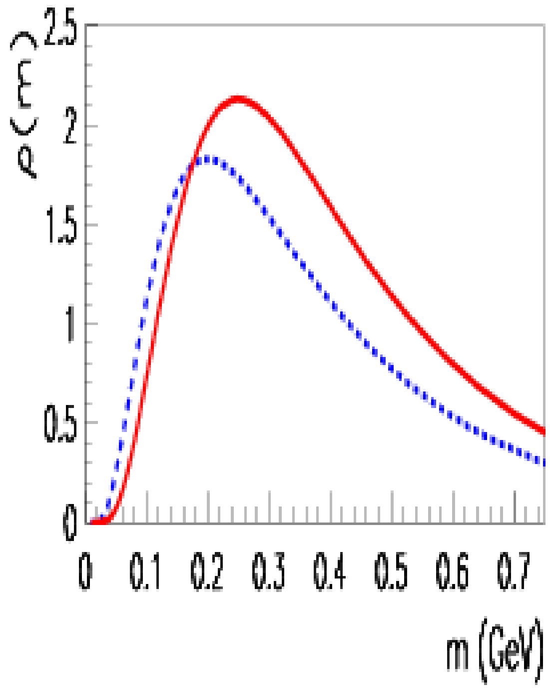


Figure 1: **Distribution of effective quark mass from eq. (1) with $\mu = 0.2GeV$ (dashed line) and $\mu = 0.25GeV$ (solid line) at $T_c = 0.26GeV$.**

**Momentum distribution of quarks**

At RHIC experiments:

**a) nearly exponential spectrum at low transverse momenta,**

**b) power-law like at high transverse momenta.**

Assume an analytic, parameterized transverse momentum distribution, which is similar to an exponential distribution for low momenta and a power law distribution for large momenta.

$$\mathbf{f_{quark}} \quad (\mathbf{p}_\perp, \mathbf{m}, \phi, \eta) = $$
$$= \quad \frac{\mathbf{A}}{[\mathbf{1} + (\mathbf{q} - \mathbf{1}) * \frac{\mathbf{E}(\mathbf{p}_\perp, \mathbf{m}, \phi, \eta)}{\mathbf{T}}]^{(\mathbf{q}/(\mathbf{q}-\mathbf{1}))}}$$

Here $q$ is a parameter characterizing a possible deviation from the usual Boltzmann distribution, which is recovered for $q = 1$. The parameter $T$ is in general not the usual temperature, but in the Boltzmann limit, $q \to 1$ it becomes the canonical temperature.

Although this expression (2) coincides with the form of the Tsallis distribution[?] (as many simple minded fits do), we do not necessarily have to assume a special equilibrium state, which is considered in the non-extensive thermodynamics.

One may assume the existence of such an equilibrium Tsallis system in quark matter if one of the following conditions is fulfilled:

**i) there is an energy dependent random noise in the system;**

**ii) the system contains a finite number of particles which interact indefinitely long;**

**iii) there are long range forces in the system.**

**We realize, that such conditions may be found in a fireball produced in high energy heavy ion collisions, it is just not sure, whether the time is enough to arrive at such a special equilibrium state.**

## Coalescence of Massive Quarks

Using the covariant coalescence model of Dover *et al.* [?], the spectra of hadrons formed from the coalescence of quark and antiquarks can be written as

$$\mathbf{E} \cdot \frac{\mathbf{dN_h}}{\mathbf{d^3p}} = \frac{\mathbf{dN_h}}{\mathbf{dyp_Tdp_Td}\phi_\mathbf{p}} = \frac{\mathbf{g_h}}{(\mathbf{2}\pi)^\mathbf{3}} \int (\mathbf{p_h^\mu} \cdot \mathbf{d}\sigma_{\mathbf{h},\mu}).\mathbf{F_h(x_h; p_h)}.$$

Here $F_h(x_h; p_h)$ is an in principle eight dimensional distribution (Wigner function) of the formed hadron. Furthermore $d\sigma$ denotes an infinitesimal element of the space-like hypersurface where the hadrons are formed, while $g_h$ is the combinatorial factor for forming a colorless hadron from a spin 1/2 color triplet quark and antiquark. For pions the statistical is $g_\pi = 1/36$ , for antiprotons $g_{\overline{p}} = 1/108$

For the $a + b \to M$ meson production the source function, $F_M(\mathbf{p}_M)$

$$\mathbf{F_M(p_h) = \int d^3p_a d^3p_b f_a(p_a; 0) f_b(p_b; 0) C_M(p_a, p_b, p_M)}. \tag{2}$$

The coalescence function $C_M(p_a, p_b, p_M)$

$$\mathbf{C_M(p_a, p_b, p_M) = \alpha_M \cdot e^{-((p_a - p_b)/P_c)^2}} \tag{3}$$

The parameters $\alpha_M$ and $P_c$ reflect properties of the hadronic wave function in the momentum representation convoluted with the formation matrix element.

Assume that $P_c$ is so small, that partons with practically zero relative momentum form a meson.

$$\mathbf{p_a} = \mathbf{p_b} = \mathbf{p_M}/2 \tag{4}$$

$$\mathbf{m_a} + \mathbf{m_b} = \mathbf{m_M} \tag{5}$$

This leads to the meson coalescence function

$$\begin{aligned} \mathbf{C_M} = \alpha_\mathbf{M} & \cdot \delta(\vec{\mathbf{p}}_\mathbf{a} - \vec{\mathbf{p}}_\mathbf{M}/\mathbf{2}) \cdot \delta(\vec{\mathbf{p}}_\mathbf{b} - \vec{\mathbf{p}}_\mathbf{M}/\mathbf{2}) \\ & \cdot \delta(\mathbf{m_a} + \mathbf{m_b} - \mathbf{m_M}) \end{aligned} \tag{6}$$

Thus we arrive at the following meson distribution function:

$$\begin{aligned} \mathbf{F_M}(\mathbf{p_t}; \mathbf{0}) &= \alpha_M \\ \cdot \int_0^{\mathbf{m_M}} \mathbf{dm_a} &\cdot \int_0^{\mathbf{m_M}} \mathbf{dm_b} \cdot \delta(\mathbf{m_M} - (\mathbf{m_a} + \mathbf{m_b})) \\ &\cdot \rho(\mathbf{m_a}) \cdot \mathbf{f_q}(\mathbf{p_t}/\mathbf{2}; \mathbf{m_a}) \\ &\cdot \rho(\mathbf{m_b}) \cdot \mathbf{f_b}(\mathbf{p_t}/\mathbf{2}; \mathbf{m_b}). \end{aligned} \tag{7}$$

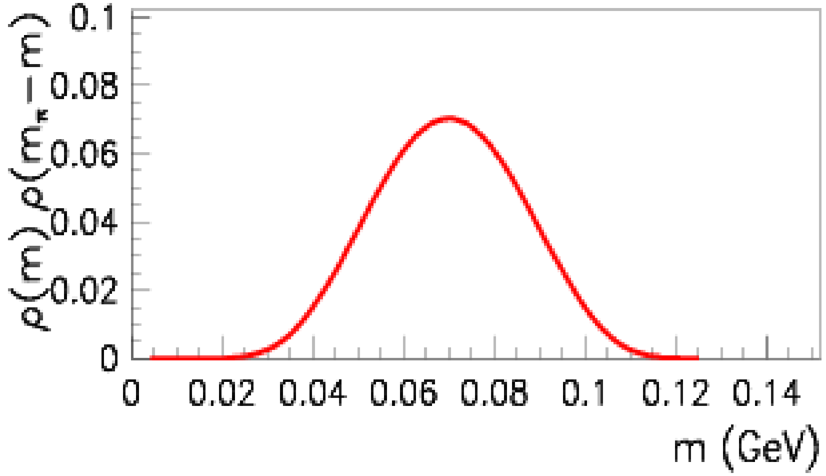


Figure 2: The product of the two quark mass distributions $\rho(m) \cdot \rho(m_\pi - m)$, eq(7). Its maximum is at $m = m_\pi/2$.

Fig.2. shows the product of two quark mass distribution functions appearing in the coalescence probability eq(7) for the coalescence production of a pion. Already the naive coalescence approach works, whenever this maximum is sharp enough.

Similar argumentation leads to the three-fold coalescence expression. In the place of eq.(5) we get:

$$\mathbf{p_1 = p_2 = p_3} = \mathbf{p_B}/3 \quad (8)$$
$$\mathbf{m_1 + m_2 + m_3} = \mathbf{m_B} \quad (9)$$

and the baryon source function becomes

$$\begin{aligned}\mathbf{F_B(p_t)} &= \alpha_B \\ &\cdot \int_0^{\mathbf{m_{pr}}} \mathbf{dm_1} \int_0^{\mathbf{m_{pr}}} \mathbf{dm_2} \int_0^{\mathbf{m_{pr}}} \mathbf{dm_3} \\ &\cdot \rho(\mathbf{m_1})\, \mathbf{f_q}(\mathbf{p_t/3, m_1})) \\ &\cdot \rho(\mathbf{m_2})\, \mathbf{f_q}(\mathbf{p_t/3, m_2})) \\ &\cdot \rho(\mathbf{m_1})\, \mathbf{f_q}(\mathbf{p_t/3, m_3}))\, \delta(\mathbf{m_B - (m_1 + m_2 + m_3)}). \quad (10)\end{aligned}$$

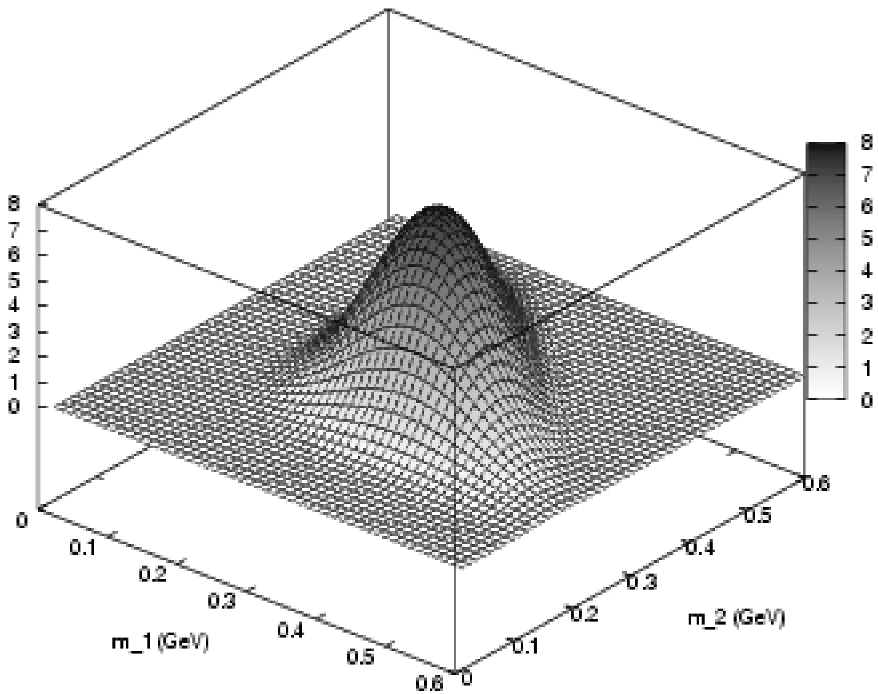


Figure 3: Product of three mass distribution, eq(10), where the X and Y axes are $m_1$ and $m_2$, and $m_3$ is defined as $m_3 = m_B - (m_1 + m_2)$.

The maximum contribution to the coalescence integrals are obtained from the equal mass part of the mass distributions.

At the end of this section we may compare the basic philosophy of the different coalescence models. In all cases we are met with the problem of mismatch of the initial and final state quantum numbers. To resolve this problem different solutions are proposed:

a) In the quantum mechanical approach the overlap of the initial and final state wave function is calculated. In this process - simply said - the quantum mechanical uncertainty bridges the mismatch gap.

b) In the most often used classical approximation the coalescence probability is smeared around the momentum conservation, Ref. [?] .

c) In the present approximation in the coalescence transition the momentum is strictly conserved, as in Ref.[?], but the masses of the particles of the initial state have a finite width distribution.

**Numerical results and comparison with experimental data**

The parameters used in the calculations are as follows. $T = 0.07$ GeV, $q = 1.19$, $v_{flow} = 0.56$, $\mu = 0.25$ GeV, $T_c = 0.26$ GeV. The $\alpha_M$ and $\alpha_B$ coalescence constants were adjusted to fit the absolute value of the measured $\pi$ and $\bar{p}$ yields. In Fig.() both the $\pi^-$ and $\pi^0$ data are displayed.

In the Figures 4-6 we show the calculated distributions together with the corresponding experimental data. The experimental points are taken from Ref. [?].

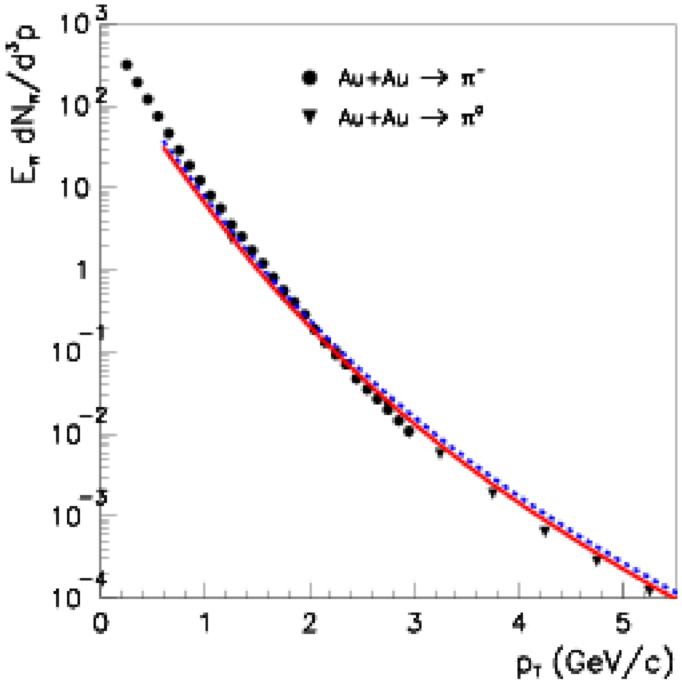

$E_\pi\, dN_\pi/d^3p$
Au+Au → π⁻
Au+Au → π⁰
$p_T$ (GeV/c)

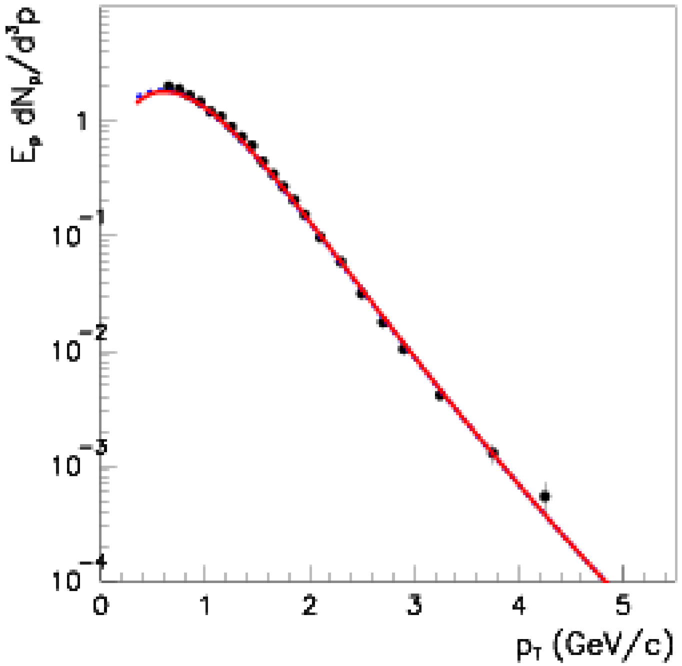
$E_p\, dN_p/d^3p$
1
$10^{-1}$
$10^{-2}$
$10^{-3}$
$10^{-4}$
0
1
2
3
4
5
$p_T$ (GeV/c)

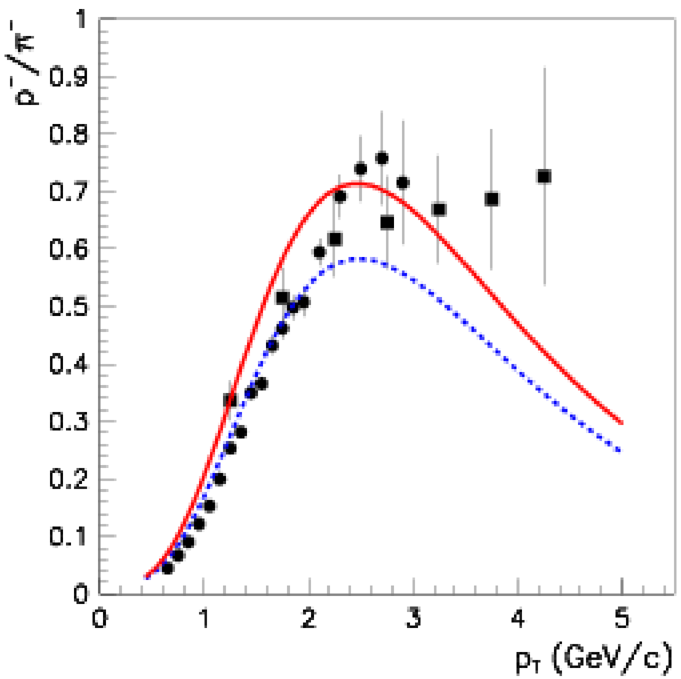
$p^-/\pi^-$
1
0.9
0.8
0.7
0.6
0.5
0.4
0.3
0.2
0.1
0
0
1
2
3
4
5
$p_T$ (GeV/c)

## Conclusion

Earlier in low, medium and high transverse momenta: thermal, coalescence and fragmentation processes.

In the present a model

a) the masses of the partons have a finite width distribution;

b)the momentum distribution of partons is described by one and the same function for a wide range of transverse momenta;

c) the hadronization happens via effective quark coalescence;

d) in the hadronization process both momentum and energy are nearly conserved locally.

# Meson and baryon elliptic flow at high $p_T$ from parton coalescence

(S.Voloshin, D.Molnár, R.J.Fries et al.)

Assymmetric quark momentum distribution:

$$\frac{dN_q}{p_\perp dp_\perp d\Phi} = \frac{1}{2\pi}\frac{dN_q}{p_\perp dp_\perp}(1 + 2v_{2,q}(q_\perp)cos(2\Phi)) \tag{1}$$

In the coalescence dynamics and for $v_2 \ll 0.1$, the hadron elliptic flow:

$$\begin{aligned} v_{2,M}(p_\perp) &\approx 2 * v_{2,q}(p_\perp/2) \\ v_{2,B}(p_\perp) &\approx 3 * v_{2,q}(p_\perp/3) \end{aligned} \tag{2}$$

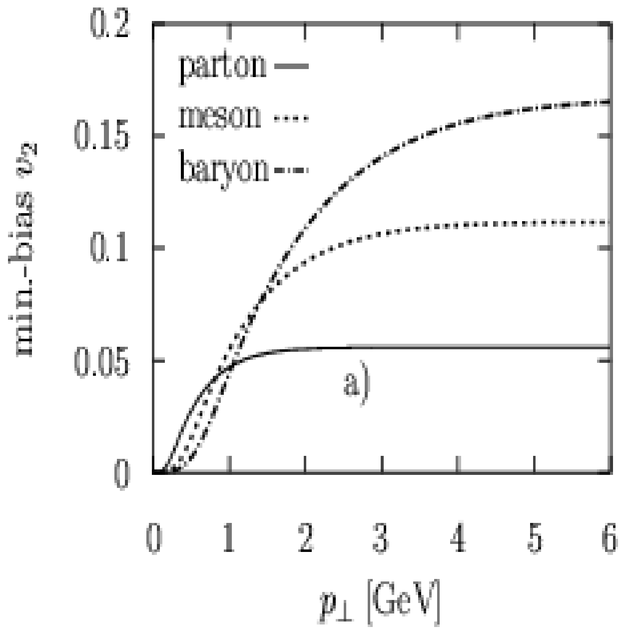


Figure 1: Qualitative shape of baryon and meson elliptic flow

* **The large and saturating differential elliptic flow $v_2(p_\perp)$ observed in $Au{+}Au$ reactions at RHIC can be explained by**

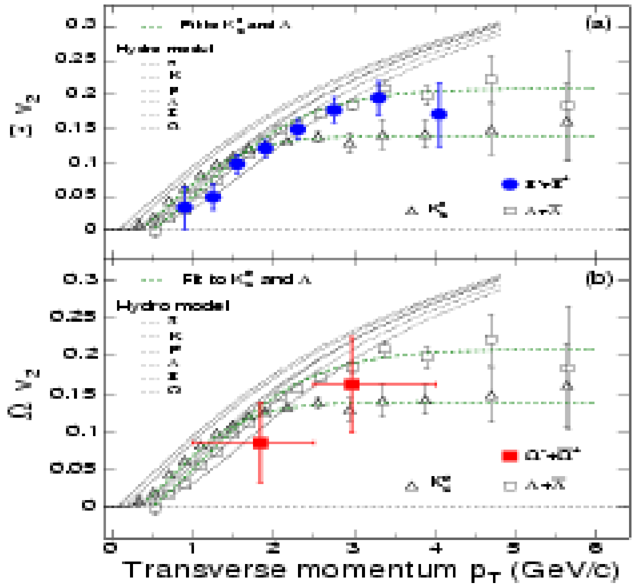


Figure 2: Measured baryon and meson elliptic flow (STAR experiment, 2005)

**hadronization via parton coalescence,**

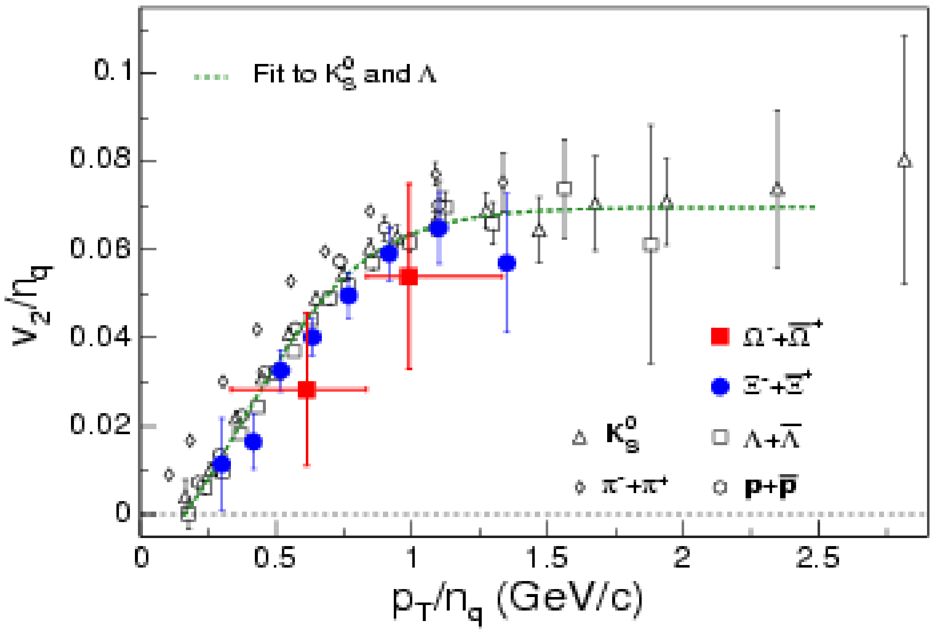


Figure 3: Measured baryon and meson elliptic flow (STAR experiment, 2005)

because it enhances hadron elliptic flow at large $p_\perp$ relative to that of partons at the same transverse momentum.

The behaviour of flow asymmetry parameter

$$v_{2,u} = v_{2,d} = v_{2,s} \tag{3}$$

implies that the

**collective flow for quarks of all flavour is the same**

**collective flow evolves during quark matter stage**

**The quarks of all flavour in this stage have an effective mass of the same order of magnitude**

(In contrast to the values of current masses.)

# CONCLUSION

**A large number of experimental fact**

**are in agreement**

with the assumption that

**in the prehadronization stage**

the quark matter consists of

**constituent quark with effective mass**

and the hadronization proceeds via

**coalescence mechanism**

the initial stage of heavy ion collision

is strong color field (gluon) dominated

the final stage of heavy ion collision

is quark dominated

# References


[1] E.Shuryak, Phys.Rept. 61, 71 (1980)

[2] T.S.Biró, J.Zimányi, Phys.Lett. 113B, 6 (1982)

[3] J.Rafelski, B.Muller, Phys.Rev.Lett. 48, 1066 (1982)

[4] T.S.Biró, J.Zimányi, Nucl. Phys. A 395, 525 (1983)

[5] T.S.Biró, P.Lévai, J.Zimányi, Phys. Lett. B 347, 6 (1995)

[6] A.Bialas, Phys. Lett. B442, 449 (1998)

[7] J.Zimányi, T.S.Biró, T.Csörgö, P.Lévai, Phys. Lett. B 472, 243 (2000)

[8] P.Lévai, U.Heinz, Phys. Rev. C 57, 1879 (1998)

[9] A.Bialas, Phys. Lett. B532, 249 (2002)

[10] M.Gyulassy, P.Lévai, I.Vitev, Nucl. Phys. B594, 371, (2001)

[11] STAR collaborararation, nucl-ex/0211024

[12] STAR collaborararation, C.Adler, Phys.Rev.Lett. 87, 112303 (2001)

[13] STAR collaborararation, H.Caines, Nucl.Phys. A 698, 112 (2001)

[14] STAR collaborararation, Van Buren, J.Phys. G 28 (2002)

[15] STAR collaborararation, P.Facchini, J.Phys. G 28 (2002)

[16] STAR collaborararation, C.Adler, Phys.Rev.Lett. 87, 262302, (2001)

[17] M.Gyulassy, L.McLerran, Nucl. Phys. A750, 30 (2005)

[18] J.Zimányi, P.Lévai, T.S.Biró, Heavy Ion Phys. 17, 205 (2003), hep-ph/0205192

[19] J.Zimányi, T.S.Biró, P.Lévai, J. Phys. G. 31, 711 (2005)

[20] R.C.Hwa, C.B. Yang Phys. Rev. Lett. 90, 212301 (2003)

[21] V.Greco, C.M.Ko, P.Lévai, Phys. Rev. Lett. 90,202302, (2003)

[22] J. Fries, S. A. Bass, B. Müller, C. Nonaka, Phys. Rev. Lett. 90:202303, (2003), nucl-th/0306027

[23] D.Molnár, S.A.Voloshin, Phys.Rev.Lett. 91:092301 (2003)

[24] STAR collaboration, J.Adams, nucl-ex/0504022